Available online at www.sciencedirect.com
ScienceDirect
Polymer 48 (2007) 183–194
polymer
www.elsevier.com/locate/polymer

The role of microstructure, molar mass and morphology on local relaxations in isotactic polypropylene. The α relaxation

Mario Hoyos, Pilar Tiemblo, José Manuel Gómez-Elvira*

Instituto de Ciencia y Tecnología de Polímeros (CSIC), Juan de la Cierva 3, 28006 Madrid, Spain

Received 19 July 2006; received in revised form 17 October 2006; accepted 16 November 2006
Available online 5 December 2006

Abstract

This study aims to assess the relative influence of microstructure, molar mass and morphology on the local α relaxation of isotactic polypropylene (iPP). For that purpose, three families of samples have been prepared. The Ziegler–Natta type provides a wide molar mass range where both the isotactic average length (n_1) and the nature of the isotacticity interruptions change according to chain size. The metallocene type allows to analyse also the samples in which molar mass and n_1 are related but the nature of the defects stays the same. Finally, three propylene-like EP copolymers (containing only isolated ethylene units) have been synthesised via metallocene catalysis in order to study samples which combine both relatively high molar masses and short n_1.

Among the factors considered, microstructure and n_1 in particular have been found to drive mainly the quality of the α relaxation. Concerning the intensity, it has been observed that some microstructural features related to n_1 must be fulfilled for this dynamics to take place. Provided this requirements are met, the intensity of the α relaxation depends on the final crystalline distribution resulting from a given molar mass, microstructure and processing conditions.

Keywords: Polypropylene; α Relaxation; Microstructure

1. Introduction

It is well known that local dynamics of chains determine the mechanical performance of isotactic polypropylene (iPP) at temperatures below 0 °C. As a matter of fact, the small scale γ relaxation drives the damping response under T_g, typically between −130 °C and 0 °C. Furthermore, local dynamics contribute also, together with the glass transition (β relaxation), to the mechanical response of this thermo-plastic at temperatures well-above room temperature. In fact, it is between 50 and 100 °C approximately when the α relaxation is active.

The implications of local dynamics features in the iPP performance are not only restricted to the mechanical behaviour, but also involve the thermo-oxidative stability of this polymer. Previous work has evidenced a relationship between the thermal stability of iPP and both α and γ relaxations [1–3]. In particular, it was observed that (i) initiation of oxidation is concomitant with a partial vanishing of the γ relaxation [2,3] and (ii) the α relaxation is associated with an abrupt change of p_0 [1], a parameter which reflects the ratio between the contents of initiating and propagating units in the thermo-oxidation [4]. From these results, it turns out that the γ relaxation is related to units which promote the thermal initiation while α relaxation is associated with a stabilisation effect. The opposite influence of both relaxations on the thermal stability of iPP has been confirmed in a recent study [5], which evidences that long degradation induction times are exhibited by iPP specimens characterized by high α and low γ relaxations, and short induction times by those iPP with low α and high γ relaxations, whatever the type (Ziegler–Natta or metallocenic), the molar mass and the microstructure may be.

Initiation of oxidative degradation is admitted to start at the inter-phase region [6]. This fact, together with the implication of both relaxations in the thermal oxidation, suggests that these dynamics are to a high extent associated with this zone. Actually, the α relaxation has been described in

* Corresponding author. Tel.: +34 915622900; fax: +34 915644853.
E-mail address: elvira@ictp.csic.es (J.M. Gómez-Elvira).

0032-3861/$ - see front matter © 2006 Elsevier Ltd. All rights reserved.
doi:10.1016/j.polymer.2006.11.034

polyethylene (PE) [7–10] and iPP [11–13], among other semi-crystalline polymers like poly(ethyleneoxide) (PEO) and poly(oxymethylene) POM [13], as a local chain motion involving both crystalline and amorphous phases. In the particular case of PE, NMR evidence of helical jumps through the inter-phase and chain diffusion within the crystals has been found [12]. This mechanism has been checked to occur also in the iPP [13], where tactic regularity is required for the segment diffusion between phases to take place.

According to this model, an influence of chain characteristics, i.e., microstructure and molar mass, and morphology, i.e., crystalline content and size distribution of crystals, on the α relaxation can be predicted. The former because they control the average length of the isotactic segments that are able to be transferred between the crystalline and the amorphous phases. The latter because some inter-chain associations could disable isotactic chain segments for such dynamics.

Three families of materials have been prepared to assess the influence of chain characteristics and morphology on the iPP local chain dynamics. Classical Ziegler–Natta iPP, metallocene iPP and metallocene polypropylene-like EP copolymers (ethylene content up to 3.3 mol%) provide a wide variety of samples to perform this study. Actually, fractionation of a commercial ZN iPP is a suitable way to obtain a family of samples that are different enough in molar mass as well as microstructure, because both characteristics are closely related due to the multiple-site catalysis followed in a heterogeneous polymerisation [14]. On its turn, metallocene catalysis is recognized to be a powerful synthetic route to tailor molar mass and microstructure in quiral polyolefins [15,16]. Finally, metallocene iso-specific copolymerisation of propylene with very low contents of ethylene, allows the preparation of the third family. The main goal of these materials is to combine high molar masses and short isotactic average lengths in the chains. The introduction of ethylene in the propylene polymerisation is known to yield random EP copolymers with an increased molar mass [17]. As a necessary consequence, isolated ethylene units contribute to reduce the isotactic average length.

2. Experimental

2.1. Samples

2.1.1. Nomenclature

The iPP samples are referred in this study according to a similar criterion that is used by Alamo et al. [18]. As in that case, each family is recognized by their corresponding initials (“ZN”, “M” and “EP” stand for Ziegler–Natta, metallocene and ethylene/propylene copolymers, respectively) followed by molar mass in kilodalton but, here, it is the isotactic average length, the number which completes the name.

2.1.2. Preparation

2.1.2.1. ZN samples. The five ZN samples correspond to four soluble and one insoluble fractions yielded by the fractionation of a commercially grade polypropylene, kindly supplied by Repsol-YPF. The original virgin polymer PP050 was purified with the solvent/non-solvent pair *o*-dichlorobenzene/acetone, at 125 °C, under N_2 and in the presence of Irganox 1010 (1 g/L). Then, it was fractionated by means of the solvent gradient extraction technique (also called direct extraction) initially developed by Holtrup [19] and according to the conditions used by Lehtinen and Paukkeri [20]. Table 1 shows the steps that are performed always under N_2 and in the presence of Irganox 1010 to avoid degradation. Only the samples selected for our study are shown in the table.

This method has been found to achieve the extraction of chains successively by isotacticity and molar mass in a specific way. In fact, previous washing with heptane removes the most atactic and low-molar mass fraction. The four subsequent steps (steps 2–5 in Table 1) with xylene/2-ethoxyethanol mixtures of decreasing polarity allow to separate chains of increasing isotacticity but in a very narrow molar mass range. Further extractions (steps 6 and 7) take place exclusively according to the molar mass and soluble fractions showing increasing molar masses and an almost constant isotacticity.

As the weight percentage extracted in every step remains very low (less than 4 wt.% for steps 1–6 and 15 wt.% for step 7), it was considered to fulfil successfully the requirements for an effective solvent gradient fractionation. Consequently, one can assume rather low polydispersities in the soluble fractions (from 2.0 to 3.5 in molar mass according to data reported by Lehtinen and Paukkeri [20]).

Sample ZN238K331 is the only insoluble fraction included in this study and a higher polydispersity can be supposed in this case.

2.1.2.2. M samples. M samples were obtained using the polymerisation procedure previously reported [5] under the conditions shown in Table 2. The combination of the metallocene catalyst type, the polymerisation temperature and the

Table 1
Purification and fractionation procedure of the PP050 sample

Step	Solvent	Vol.%	Temp. (°C)	Non-solvent	Soluble fraction	Insoluble fraction
Purification	*ortho*-Dichlorobenzene	100	125	Acetone	Repsol-YPF-PP050	
1	Heptane	100	40	Acetone	–	–
2	Xylene/2-ethoxyethanol	30/70	125	Acetone	–	–
3	Xylene/2-ethoxyethanol	40/60	125	Acetone	–	–
4	Xylene/2-ethoxyethanol	50/50	125	Acetone	ZN46K19	–
5	Xylene/2-ethoxyethanol	60/40	125	Acetone	ZN47K78	–
6	Xylene/2-ethoxyethanol	70/30	125	Acetone	ZN64K220	–
7	Xylene	100	125	Acetone	ZN205K498	ZN238K331

Table 2
Polymerisation conditions for M samples

Sample	Solvent	Catalyst/co-catalyst	[Al]/[Zr]	Propylene pressure (bar)	Temp. (°C)
M182K131	Toluene	$Si(CH_3)_2[Ind]_2ZrCl_2$/MAO	1639	2	−10.0
M145K78	Toluene	$Si(CH_3)_2[Ind]_2ZrCl_2$/MAO	1639	2	−10.0
M128K48	Toluene	$Si(CH_3)_2[Ind]_2ZrCl_2$/MAO	1639	2	−5.0
M125K22	Toluene	$Et[Ind]_2ZrCl_2$/MAO	1529	2[a]	−36.6
M88K31	Toluene	$Et[Ind]_2ZrCl_2$/MAO	1529	2	−18.5
M80K41	Toluene	$Et[Ind]_2ZrCl_2$/MAO	1529	2	−10.0
M65K21	Toluene	$Et[Ind]_2ZrCl_2$/MAO	1529	2	−5.0
M55K22	Toluene	$Et[Ind]_2ZrCl_2$/MAO	1529	2	−33.0
M47K23	Toluene	$Et[Ind]_2ZrCl_2$/MAO	1529	2	−5.0
M36K15	Toluene	$Et[Ind]_2ZrCl_2$/MAO	1529	2	−20.0
M29K28	Toluene	$Et[Ind]_2ZrCl_2$/MAO	1529	2	30.0
M23K25	Toluene	$Et[Ind]_2ZrCl_2$/MAO	1529	2	30.0
M16K26	Toluene	$Et[Ind]_2ZrCl_2$/MAO	862	2[a]	30.0

[a] The reaction was allowed to continue without restoring the initial monomer pressure of 2 bar.

catalyst/co-catalyst ratio allows to obtain a variety of polymers in a wide molecular weight range, between 16 000 and 182 000 Da. *rac*-Ethylenbis(indeyl)zirconium dichloride was used to obtain M samples with molar masses from 125 000 Da downwards and *rac*-dimethylsylilbis(indeyl)zirconium dichloride, in combination with a higher [Al]/[Zr] ratio, for the three highest molar masses 128 000, 145 000 and 182 000 Da. These two classical metallocene polymerisations yield PE and iPP samples with polydispersities very much close to 2 [21]. Catalyst traces were removed by pouring the reaction medium into a CH_3OH/HCl (5 vol.%) mixture. Finally, polymers were filtered, washed with CH_3OH and dried under vacuum at room temperature. All M samples were used without any further purification.

2.1.2.3. EP samples. As indicated in Table 3, the EP copolymers were synthesised using identical conditions to the polymerisation of M65K21 (Table 2). In this case the reactor was fed with an ethylene/propylene mixture which kept the reaction pressure at a constant value of 2 bar. The mixture of both co-monomers was kept in a stainless steel cylinder, at ambient temperature and at a total maximum pressure of 7 bar to avoid the liquation of propylene.

2.1.3. Processing

Original iPP materials have been obtained as fine powders in all cases. This aggregation state results from the precipitation of chains either in solution (soluble ZN fractions) or in a more or less swollen gel (the M and EP series and the insoluble ZN fraction). The powders were compacted by compression-moulding so as to obtain the required samples for the dynamo-mechanical and thermal analysis.

The normalization of the thermal history is a necessary requisite for the comparison of the samples' final properties. Consequently, processing conditions have been chosen following the criterion of giving the same opportunity of ordering from the above mentioned quenched status. For such purpose, quantity (80 mg), mould dimensions ($150 \times 4 \times 0.5$ mm) and processing pressure and time (190 bar and 3 min, respectively) were unchanged, but the temperature was varied according to the characteristics of the powder's global crystallinity as it is shown by the corresponding DSC curve. In particular, the set-up temperature of the endotherm was taken. This processing resembles a crystallization performed from disordered chains in the melt at equivalent under-cooling values.

2.2. Characterisation

2.2.1. Molar mass

The viscosimetric average of the molar mass was calculated from the intrinsic viscosity of polymers, using the Mark–Howink relationship $[\eta] = 11 \times 10^{-3}\,Mv^{0.8}$ which corresponds to the isotactic polypropylene dissolved in decaline at 135 °C [22]. This equation was considered to be valid for the three EP copolymers because of their very low ethylene content.

2.2.2. Anomalous chemical groups content

The relative content of anomalous chemical functions, namely double bonds and carbonyl groups, was estimated by means of the infrared spectra of polypropylenes in the region 1530–1800 cm^{-1} normalised to the 2720 cm^{-1} band. The

Table 3
Polymerisation conditions of EP samples

Sample	Solvent	Catalyst/co-catalyst	[Al]/[Zr]	Feeding mixture ethylene/propylene (bar ratio, $\times 10^3$)	Reaction pressure (bar)	T (°C)
EP99K43	Toluene	$Et[Ind]_2ZrCl_2$/MAO	1529	0.75	2.0	−5.0
EP94K28	Toluene	$Et[Ind]_2ZrCl_2$/MAO	1529	1.01	2.0	−5.0
EP120K19	Toluene	$Et[Ind]_2ZrCl_2$/MAO	1529	1.51	2.0	−5.0

spectra were recorded on hot-pressed films using a FTIR Perkin–Elmer Spectrum-One, 10 scans and 2 cm^{-1} resolution. Comparison of the FTIR spectra shows that no significant differences were found as regards the type and the amount of oxygenated and double bond groups.

2.2.3. Crystallinity and melting point

The DSC measurements have been carried out in a Perkin–Elmer DSC-7 calorimeter with about 5 mg of sample cut from the processed samples, and scanning between 40 °C and 210 °C at variable heating rates (2.5, 10.0 and 20.0 °C/min) and under N_2 flow. Only the first scan has been considered in the determination of the melting temperature (T_m), the crystallinity degree (χ_c) and the endotherm shape which characterises the crystallinity of the samples resulting from the compaction process. The standard heat of melting for a 100% crystalline PP used in crystallinity calculations was 209 J/g [23].

The small portion put aside in each processed sample for the DSC analysis makes essential to check the homogeneity of the probes. In this respect, the DSC scans performed on different pieces, taken all along the probes, have confirmed the homogeneity of the processed materials. As an example, Fig. 1 shows for EP99K43 that no relevant differences are found even when portions from different probes are compared. The thermal characteristics of the DSC curves displayed in Fig. 1 are summarised in Table 4.

Most of the probes have been checked to be close to the definite morphologies, because no melting-recrystallization processes have been detected by means of changing the scan speed in the DSC runs. However, in few cases some melting-recrystallization phenomenon takes place. Actually, Fig. 2 shows two examples for each situation. For EP99K43 and M47K23, the relative contribution of both DSC components remains around a constant value, when the heating rate is

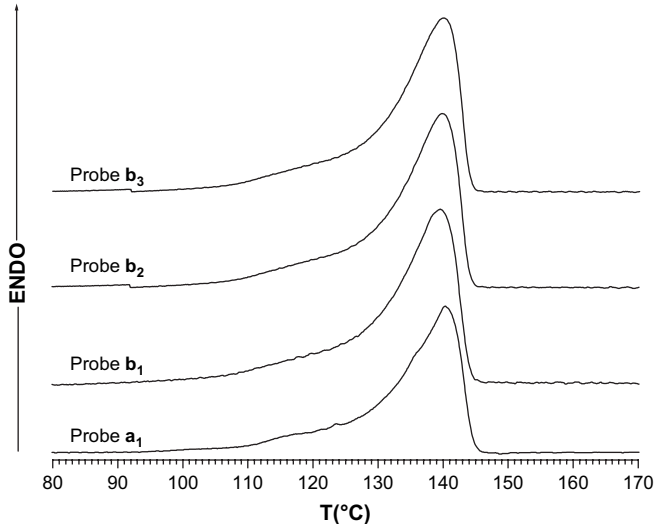

Fig. 1. DSC curves of the processed EP99K43 sample: "a" and "b" indicate different probes and sub-indexes distinguishing different portions from the same probe.

Table 4
DSC characteristics of EP99K43 obtained at 10 °C/min on 5 mg portions taken from two different probes

Sample	Probe	Portion	T_m (°C)	χ_c (wt.%)	Low-T_m fraction (wt.%)
EP99K43	a	1	140.5	39.9	50.5
	b	1	139.4	44.4	49.2
	b	2	139.7	44.2	50.5
	b	3	139.8	44.9	48.3

increased from 2.5 to 20 °C/min. On the contrary, for ZN238K331 and M182K131 the presence of small contents of non-equilibrium crystallites is apparent according to the lower contribution of the first melting process at 2.5 °C/min. Nevertheless, the variations in the relative area of the low-T_m shoulder at 10 and 20 °C/min are within the experimental error. Then, recrystallization seems to be suppressed at a heating rate of 10 °C/min, as it has been observed by Iijima and Strobl [24]. As a consequence, the endotherm's shape obtained at 10 °C/min reflects the melting of the original crystalline distribution in the processed samples and they have been used to evaluate the relative contribution of the low-T_m peak. Contributions of the low-T_m crystalline phase in ZN, M and EP samples are shown in Tables 5–7, respectively, together with global crystalline contents and melting temperatures.

The fraction of low-T_m crystals in each sample was obtained from the relative area under the low-temperature shoulder of the endotherm. The calculation implies first the deconvolution of the DSC curve as it has been described previously [25] and second, the integration of every single component placed from $T_{max} - 7$ °C downwards as a whole. Such temperature has been established empirically from the fact that the main melting peak can be always built from two or three components placed at temperatures higher than $T_m - 7$ °C. This criterion is supported by data reported by Auriemma and De Rosa [26] and Iijima and Strobl [24]. Provided that the melting-recrystallization process is negligible, the former find that the separation between the two melting peaks can be less than 10 °C and, the latter specifically propose the existence of three regimes which imply the successive melting of transverse, subsidiary and main parent lamella. The temperature which defines the transition to the final melting of the most stable crystals being $T_m - 8$ °C.

2.2.4. Mechanical relaxations

The loss modulus (E'') spectra obtained from the dynamic thermo-mechanical analysis provide the temperature values and the intensities of the α, β and γ mechanical relaxations of the samples. They were obtained with a Thermal Instrument DMA 983 analyzer, in flexion mode, from the samples processed under the conditions mentioned before. The frequency of oscillation was 0.1 Hz, the temperature range from −150 °C to 130 °C, the heating rate 5 °C/min and the deformation amplitude 0.8 mm.

The relative intensities of the α, β and γ relaxations were calculated by measuring the corresponding relative areas

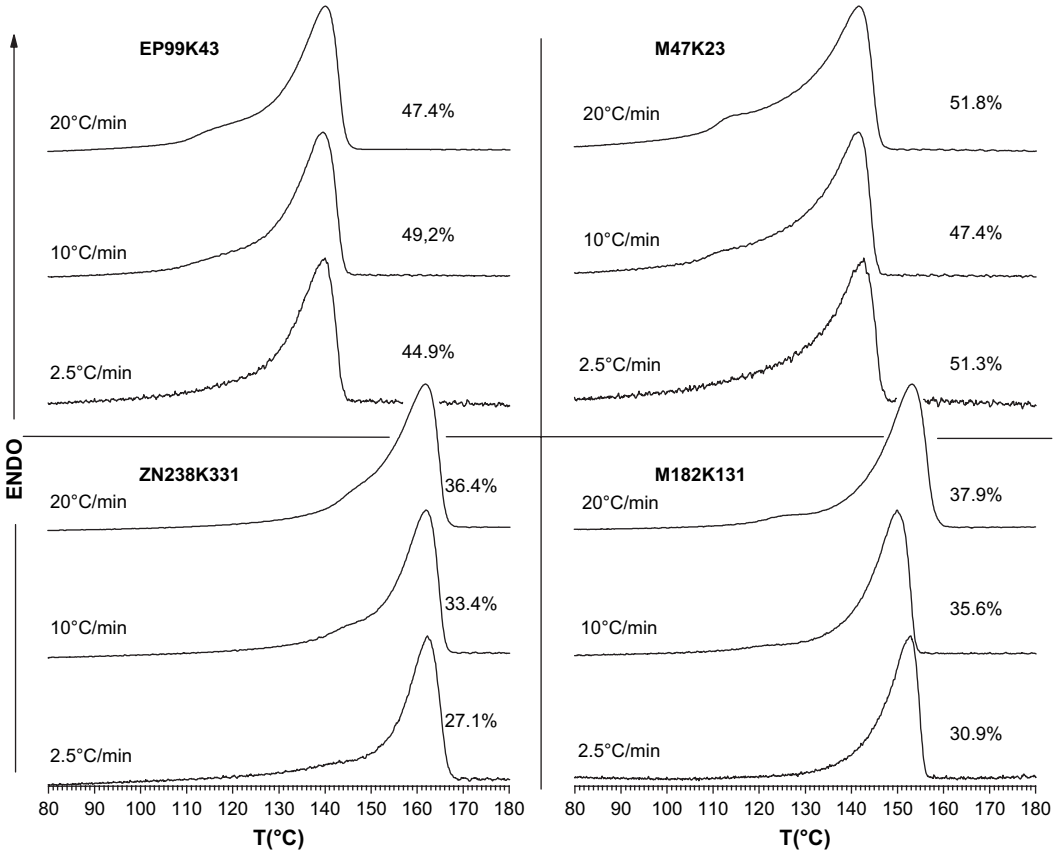

Fig. 2. DSC curves at different heating rates of some processed samples. The contribution of the low-T_m crystalline phase is indicated in each case.

Table 5
DSC characteristics of ZN samples

Sample	T_m (°C)	χ_c (wt.%)	Low-T_m fraction (wt.%)
ZN238K331	166.6	54.1	34.8
ZN205K498	162.0	54.6	44.5
ZN64K220	161.1	55.2	37.8
ZN47K78	158.2	47.5	40.1
ZN46K19	144.9	29.8	51.0

Table 6
DSC characteristics of M samples

Sample	T_m (°C)	χ_c (wt.%)	Low-T_m fraction (wt.%)
M182K131	152.3	52.2	27.3
M145K78	–	–	–
M128K48	150.1	49.0	29.9
M125K22	150.8	39.6	50.5
M88K31	145.5	39.6	35.9
M80K41	145.9	44.5	35.4
M65K21	143.6	41.5	45.6
M55K22	146.8	37.4	53.5
M47K23	142.8	37.2	55.8
M36K15	143.5	35.4	56.5
M29K28	137.4	45.3	33.7
M23K25	137.1	42.5	54.3
M16K26	146.0	40.4	43.9

Table 7
DSC characteristics of EP samples

Sample	T_m (°C)	χ_c (wt.%)	Low-T_m fraction (wt.%)
EP99K43	140.5	39.9	50.5
EP94K28	136.7	46.1	47.0
EP120K19	134.2	39.3	47.2

from the deconvoluted E'' spectra, as performed in earlier work [3].

2.2.5. Microstructure

Tactic microstructures of samples were calculated, in terms of triad percentages, from the methyl signals in the ^{13}C NMR spectra. They are shown in Tables 8–10 for ZN, M and EP families, respectively. Regio-irregular insertions of the 2,1-erythro and threo types were measured also by means of their corresponding methyl signals. Other anomalous structures as 1,3-insertions have been only detected in the three lowest molar mass M polymers, but in a negligible concentration.

The calculation of the P**P**P(*mr*) triad content was performed by subtracting the contribution of the as-named methyl type 2 defined by other authors [27]. This particular signal corresponds to the configuration of the last regio-regular propylene unit inserted in the growing chain, before a regio-irregular 2,1 insertion takes place. The peculiarity of such an unit is

Table 8
Microstructure of ZN samples as obtained by ^{13}C NMR

Sample	PPP				PPP regio-irregular (%)	n_1[a]	Microstructure type[b]
	% (mm)	% (mr)	% (rr)	mr/rr			
ZN238K331	99.1	0.6	0.3	2.0	0	331	PP(r_2)
ZN205K498	99.4	0.4	0.2	2.0	0	498	PP(r_2)
ZN64K220	98.7	0.9	0.4	2.2	0	220	PP(r_2)
ZN47K78	95.8	2.5	1.7	1.5	0	78	PP($r_{>2}$)
ZN46K19	81.6	9.1	9.3	1.0	0	19	PP($r_{>2}$)

[a] Calculated taken into account that [Interruptions] = [mr].
[b] According to Scheme 1.

a $-CH(CH_3)-$ group adjacent to a two methylene segment, whose methyl resonance overlaps with those ones corresponding to P**P**P(*mr*) units. They are referred in Table 9 as P**P**P(mm_2) and they have been theoretically estimated as the half of the regio-irregular methyl signals.

In the case of the EP copolymers, propylene units giving $-CH(CH_3)-$ groups isolated from the adjacent isotactic segments by more than one methylene group have been detected. These units have been identified either as real isolated propylene units (PE**P**EP-m_3m_3) or as configurations produced from consecutive regio-irregular propylene and ethylene insertions (P**P**EP-m_2m_2) [28]. The high sensitivity of the methyl region to configurational differences makes it difficult to measure accurately the low intensity signals, because they appear as small areas spreading over a rather wide range of ppm. For such a reason, the contents of isolated methyl groups were better evaluated from the associated methine resonances. In particular, $T_{\delta\delta}$ for PE**P**EP(m_3m_3) and $T_{\beta\gamma}$ for **P**PE**P**(m_2m_2) [28]. Isolated methyl groups are referred in Table 10 as a whole.

Tables 8–10 also show the isotactic average lengths (n_1) as they were obtained from the total content of the isotacticity interruptions using the expression $n_1 = ([mm] + 0.5[mx])/0.5[mx]$, where the nature of the interruptions (mx) is indicated in each of the tables. In the case of the EP copolymers, the ethylene content was obtained from the methylene signals according to the following expression:

$$\text{mol\% (ethylene units)} = \frac{1/2\int(\text{ethylene-CH}_2)}{1/2\int(\text{ethylene-CH}_2) \oplus \int(\text{propylene-CH}_2)}$$

The calculus of the methylene fraction which belongs to propylene and ethylene units was performed as it is proposed by Cheng [28].

Spectra were run on a Varian Unity 500 spectrometer operating at 125.708 MHz in d_2-tetrachloroethane (100 mg/mL), at 125 °C for samples with molar masses equal to or higher than 47 000 Da and at 90 °C for molar masses under this value. The acquisition time was 1 s, the relaxation delay 4 s, the pulse angle 90° and at least 8000 scans were accumulated.

Table 9
Microstructure of M samples as obtained by ^{13}C NMR

Sample	PPP				PPP regio-irregular (%)	PPP % (mm_2)	n_1[a]	Microstructure type[b]
	% (mm)	% (mr)	% (rr)	mr/rr				
M182K131	97.8	1.2	0.6	2.0	0.3	0.1	131	PP(r_2-2,1)
M145K78	96.3	1.8	0.9	2.0	0.7	0.3	78	PP(r_2-2,1)
M128K48	94.0	3.3	1.6	2.1	0.7	0.4	48	PP(r_2-2,1)
M125K22	84.8	8.2	6.9	1.2	0	0	22	PP($r_{>2}$)
M88K31	90.6	5.5	3.0	1.8	0.6	0.3	31	PP(r_2-2,1)
M80K41	93.1	3.9	1.8	2.2	0.8	0.4	41	PP(r_2-2,1)
M65K21	86.6	7.7	4.1	1.9	1.1	0.5	21	PP(r_2-2,1)
M55K22	87.4	6.7	3.4	2.0	1.7	0.8	22	PP(r_2-2,1)
M47K23	88.1	7.1	3.5	2.0	0.9	0.4	23	PP(r_2-2,1)
M36K15	82.5	8.9	4.9	1.8	2.5	1.2	15	PP(r_2-2,1)
M29K28	90.3	5.4	2.4	2.2	1.3	0.6	28	PP(r_2-2,1)
M23K25	89.0	6.0	2.9	2.1	1.4	0.7	25	PP(r_2-2,1)
M16K26	89.4	5.8	3.0	1.9	1.2	0.6	26	PP(r_2-2,1)

[a] Calculated taken into account that [Interruptions] = [mr] + [regio-irregular PPP].
[b] According to Scheme 1.

Table 10
Microstructure of EP samples as obtained by ^{13}C NMR

Sample	Ethylene	PPP				PPP regio-irregular (%)	PPEP (%)	Isolated methyls (%)	n_1[a]	Microstructure type[b]
	(%)	% (mm)	% (mr)	% (rr)	mr/rr					
EP99K43	0.6	93.8	2.7	1.3	2.1	0	1.8	0.4	43	PP(r_2-E)
EP94K28	1.1	91.2	3.4	1.6	2.1	0	3.4	0.4	28	PP(r_2-E)
EP120K19	3.3	87.6	3.5	1.6	2.2	0	6.2	1.1	19	PP(r_2-E)

[a] Calculated taken into account that [Interruptions] = [mr] + [PPEP].
[b] According to Scheme 1.

Although proton broad band decoupling was used, the NOE effect on the different tactic methyl groups was assumed to be the same [29] and a quantitative valuation of the configurational microstructure could be performed.

3. Results and discussion

3.1. Relationship between microstructure and molar mass

Fig. 3 shows the ^{13}C NMR spectra of the ZN family. As expected, the fractions of the commercial ZN iPP show a characteristic molar mass/microstructure relationship because of the multi-site nature of the heterogeneous catalyst used.

A conspicuous evolution of the configuration takes place when decreasing the molar mass from ZN238K331 to ZN46K19. The quality of the isotacticity interruptions changes, turning from exclusively isolated syndiotactic triads in the molar mass range 238–64 K to prevailing syndiotactic interruptions longer than a triad in ZN46K19. This evolution is clearly monitored through the [mr]/[rr] ratio in Table 4. PP(r_2) and PP($r_{>2}$) will stand for these two types of microstructure qualities, respectively, and they are represented in Scheme 1. The microstructure of the M samples is depicted in the ^{13}C NMR spectra shown in Fig. 4. A bigger similarity between the spectra profiles exists in spite of the wide molar mass range. In fact, most of the M polymers could be considered as PP(r_2) chains, according to the [mr]/[rr] value around two (Table 5), but because of the presence of the regioirregular 2,1-insertions they have been classified as a different microstructure quality (PP(r_2-2,1) chains in Scheme 1).

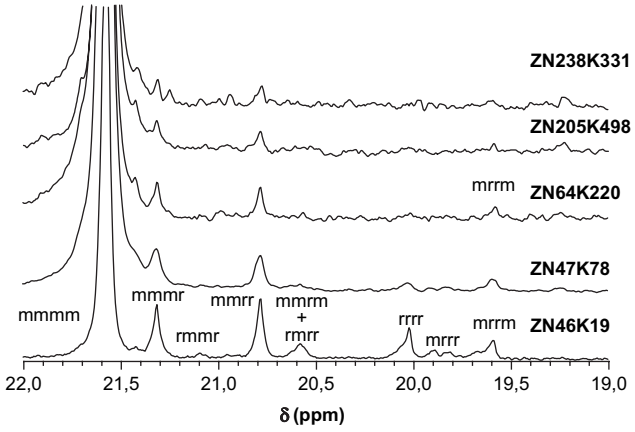

Fig. 3. ^{13}C NMR spectra of ZN samples performed at 125 °C in d_2-tetrachloroethane.

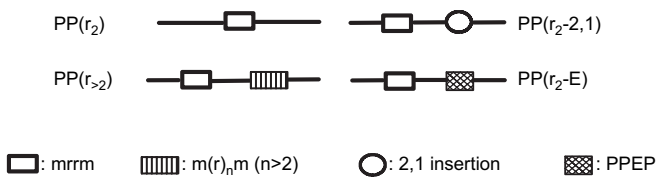

Scheme 1. Types of microstructures in the iPP samples studied.

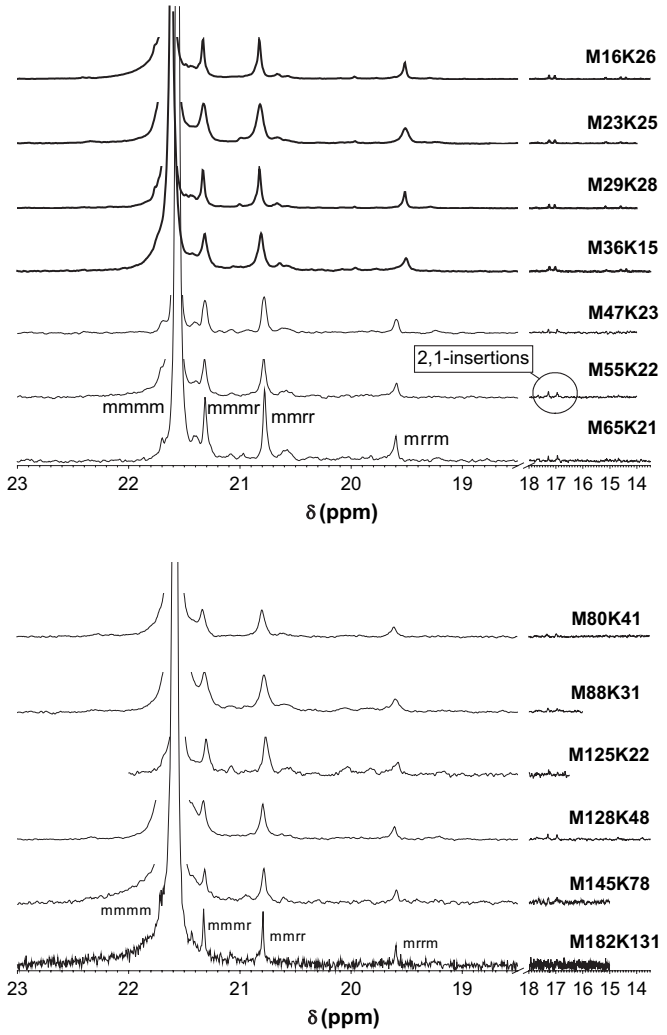

Fig. 4. ^{13}C NMR spectra of M samples performed at 125 °C (thin lines) or 90 °C (thick lines) in d_2-tetrachloroethane.

Any deviation from this PP(r_2-2,1) chain must be ascribed to the influence of particular polymerisation conditions, as is the case of M125K22 which was synthesised at both low temperature and low monomer concentration. This M sample has a clear PP($r_{>2}$) microstructure as in the case of ZN46K19. These two polymers are then examples of chains with almost identical qualitative microstructures ([mr]/[rr] ratios around 1 and no regiodefects) but very different in molar mass.

Finally, the insertion of very low contents of isolated ethylene units in the iPP chains, via metallocene copolymerisation, provides another type of polypropylene-like microstructure, if we still classify the quality of chains depending only on the nature of the defects and not on the molar mass. Fig. 5 displays the ^{13}C NMR spectra of this so-called PP(r_2-E) type chains in Scheme 1, which are free from PPP regiodefects and contain *mrrm* ([mr]/[rr] ratio about 2 in Table 6) and PPEP interruptions.

These three EP copolymers exhibit molar masses higher than M65K21, which was synthesised under identical reaction conditions. This fact is also a well-described effect due to the presence of ethylene in the metallocene iPP polymerisation [17].

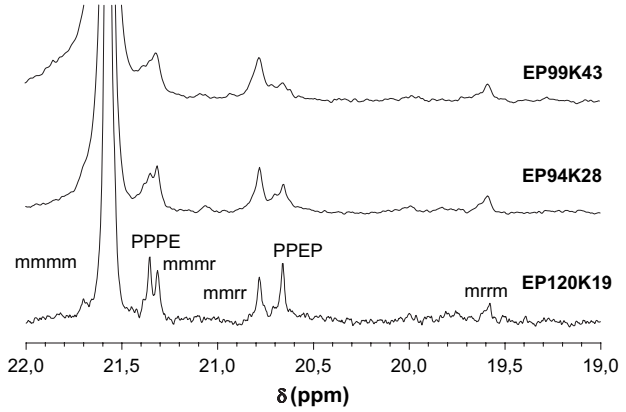

Fig. 5. ^{13}C NMR spectra of EP samples performed at 125 °C in d_2-tetrachloroethane.

We are aware of the simplification assumed proposing the classification of microstructures given in Scheme 1. It is well known that properties of ZN iPP cannot be rationalized in terms of microstructure because of their wide inter-chain heterogeneity in tacticity distribution. However, the fractionation method used assures rather low polydispersed ZN fractions in both molar mass and microstructure. We considered it interesting to first check if correlations between mechanical relaxation characteristics and the average microstructure in ZN and M samples deviate from one another; second, to explore if local mechanical relaxation above T_g obeys shared morphological reasons in both families.

3.2. Influence of molar mass and microstructure on the content of low-T_m crystals

Fig. 6 shows that the fraction of low-T_m crystals roughly correlates with molar mass in a way which confirms a special contribution of short chains to less stable lamellae, in particular for molar masses under 65 000 Da in M samples. The formation of low-T_m crystals is particularly favoured in M125K22 and EP samples, and not in two low-molar mass cases (M29K28 and M16K26). ZN samples follow roughly the same correlation with molar mass but the two most regular samples present relatively high contents of low-T_m crystals.

Although there is no unique trend when the content of low-T_m crystals is plotted against n_1, clear correlations are apparent for ZN and M polymers. Fig. 7 shows that microstructure drives greatly the crystalline distribution in metallocenic samples, which shows a strong increase of the relative content of low-T_m crystals for n_1 under 30.

As for the ZN family, a similar trend can be drawn converging with the M case at short n_1 values. The ZN lay above their metallocenic counterparts. No definitive account can be given for the ZN behaviour relative to the M evolution, but lower molar masses for similar n_1 values in ZN47K78 and ZN64K220 and a high regularity in ZN205K498 and ZN238K331 can be invoked. On the latter, particular crystallization conditions would favour the formation of low-T_m crystals in high regular iPP chains. This observation is inferred from the observation of Alamo et al. [30] who reported an unexpectedly high content of cross-hatching in an almost perfect ZN iPP fraction crystallized at high temperatures.

The typical double endotherm shown by DSC in any of the samples does not give any information about the quality of the crystals, but it is admitted to reflect the great complexity of the crystallization behaviour of iPP, which is unique among semi-crystalline polymers. Usually, the high-temperature main peak corresponds to the melting of parent lamella which has crystallized in the α polymorph. The low-temperature component arises from the melting of less stable crystals either epitaxially grown in the transverse direction to the radius of the spherulites [31,32] or subsidiary along the radial axis [24]. In addition, one must take into account the polymorphic behaviour of the iPP which depends on the molar mass, content and type of chain defects and processing conditions

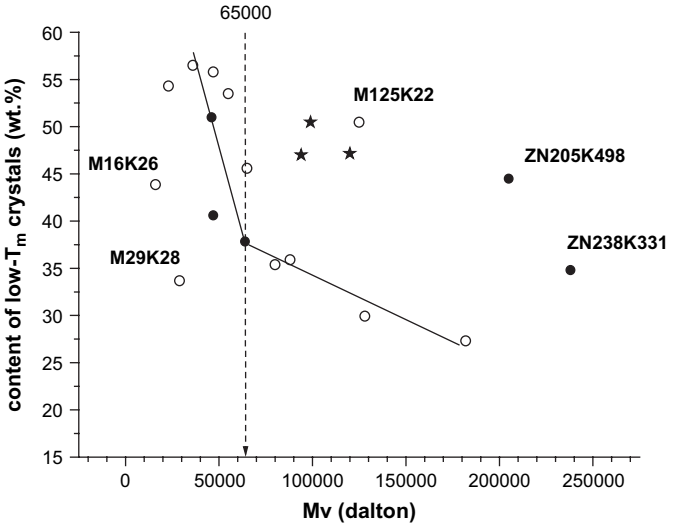

Fig. 6. Evolution of the low-T_m crystals content with molar mass for: (○) M, (●) ZN and (★) EP samples.

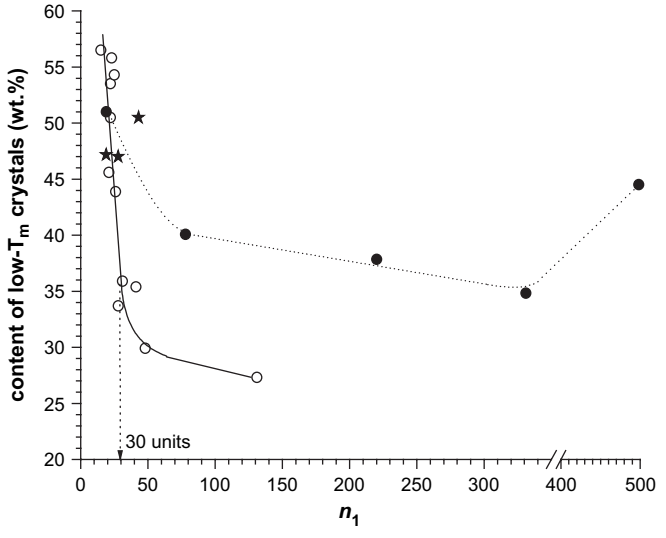

Fig. 7. Evolution of the low-T_m crystals content with n_1 for: (○) M, (●) ZN and (★) EP samples.

[18,33–35]. Apart from the β polymorph which is produced under special conditions, the γ orthorhombic system is usually associated with epitaxial crystals in metallocenic iPP samples [18,35]. However, if stereo-regularity becomes very high, iPP chains, either ZN or M, crystallize exclusively as an α polymorph whatever the lamellar quality they may produce [30,36]. The variety in the ordering quality is even wider according to the work by Auriemma et al. [26,34] who propose structurally disordered γ lattices because of the coexistence with the typical packing of the α form.

For the purpose of this study the ensemble of less stable crystals has been considered as a whole in the first approach, without distinguishing the polymorph type and the placement in the spherulite. Anyway, a different influence of the low-T_m crystals on the α relaxation process can be expected depending on whether they are epitaxial or radial.

3.3. Influence of crystallinity and microstructure on the DMA spectrum

Molar mass, microstructure and morphology must be taken into account to understand the mechanical response of the iPP materials. The analysis of DMA spectra of the samples reveals particular features which can be tentatively associated either with special morphologies or with the microstructure as it has been classified in Scheme 1.

Fig. 8 shows representative DMA examples of each one of the microstructures. The crystalline content is also indicated. As regards PP(r_2) chains, the two ZN samples are shown for comparison. It is evident that the α relaxation in ZN238K331 and ZN205K498 samples has the same position but different intensities in spite of their coincident microstructure type, total crystalline content and quite similar molar masses. As it is indicated in their names, the difference lies on the n_1 value which is much higher in the ZN205K498 polymer. Consequently, although a similar quality of the relaxation must be admitted, the important reduction of the structures which fulfil the requirements for such a dynamic in ZN205K498 can be reasonably attributed to differences in either n_1 or crystalline distribution, or both. In fact, a difference of about 10% in the low-T_m crystalline fraction between these two samples is apparent from Figs. 5 and 6.

For the rest of the microstructures, the intensity of the α relaxation can be high if the crystalline content remains important, as in PP(r_2-2,1) type, diminish in the PP(r_2-E) sample when the crystallinity lowers, and even be zero for PP($r_{>2}$) in spite of the similar crystalline content to the PP(r_2-E) case. However, T_α appears in all cases clearly around a lower value (57 °C or close to) than in the case of the PP(r_2) ZN polymers, as a characteristic of the metallocene samples. Then, a high T_α and a low T_α groups can be considered whose main difference is the n_1 value which is drastically shortened when passing from the former to the latter.

For the case of PP($r_{>2}$) one should invoke the crystalline distribution or a special influence of the defect type or both to explain the absence of α relaxation, considering that the similarity with the PP(r_2-E) includes molar mass, crystallinity and n_1.

3.4. Molar mass and microstructure dependence of the α relaxation

T_α has been found to increase with molar mass in the three iPP families. Fig. 9 shows that this trend is particular for each family, although ZN and M evolutions share a step-like shape. This feature leads to think about another factor, associated with molar mass, which makes the quality of the α relaxation to change. It is also clear that some M samples (M16, M23, M29 and M125) cannot be included in the fitting.

A unified evolution is observed when T_α is represented as a function of microstructure (Fig. 10). This dependence confirms a relation of the α relaxation with n_1 as a feature which conditions the temperature of motions irrespective of the nature of the defects.

Three well-defined n_1 ranges are observed in Fig. 10. First, T_α increases strongly when n_1 increases up to 30 units.

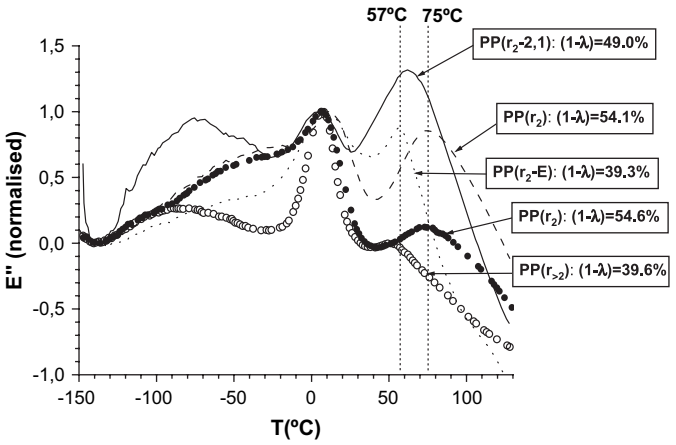

Fig. 8. DMA spectra of (---) ZN238K331; (—) M128K48; (○) M125K22; (···) EP120K19; (●) ZN205K498.

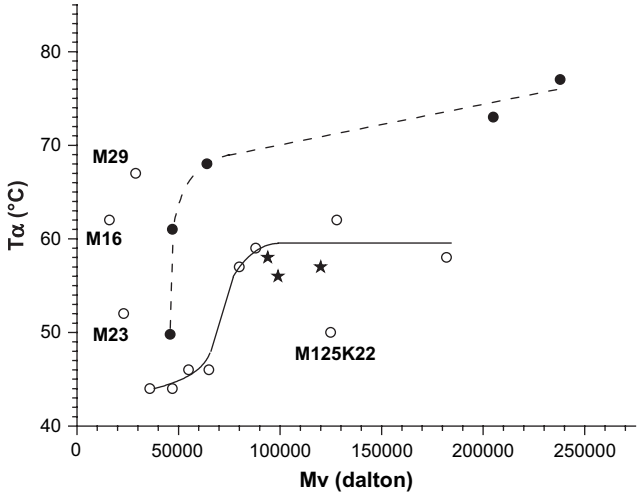

Fig. 9. Evolution of T_α with molar mass: (○) M samples; (●) ZN samples; (★) EP samples.

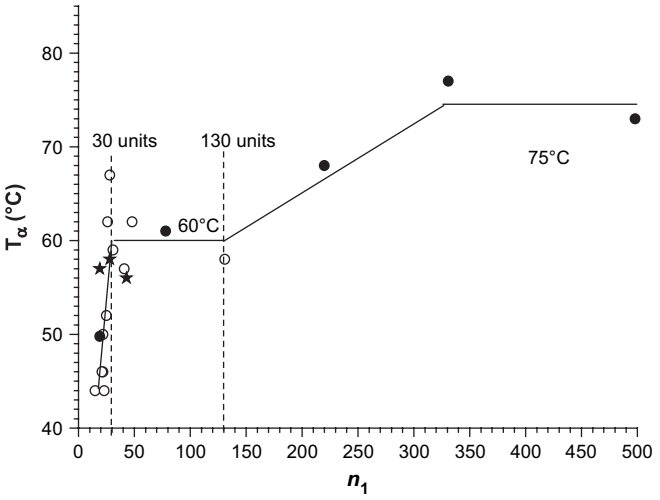

Fig. 10. Evolution of T_α with n_1: (○) M samples; (●) ZN samples; (★) EP samples.

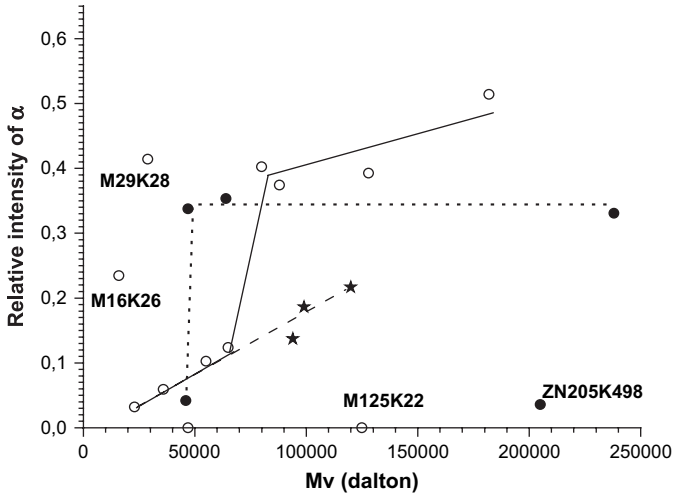

Fig. 11. Evolution of the relative intensity of the α relaxation with molar mass: (○) M samples; (●) ZN samples; (★) EP samples.

Second, from 30 units onwards, T_α reaches a plateau around 60 °C and, finally, above 130 units T_α build-up to a plateau around 75 °C. While the first range under 30 can be reasonably thought to arise from the sudden appearance of the α relaxation in the polymers which fulfil a minimum n_1 for this relaxation to take place, the successive plateaus above 30 units reflect two different relaxation qualities (mechanism or entities involved). As a matter of fact, the existence of two α relaxation processes in PE and iPP is well known [7,9,37,38] and could be due to a change of the α relaxation mechanism, as some authors have claimed [37].

According to this opinion, a low-temperature α relaxation connected with motions in the inter-lamellar zone would be the characteristic motion associated with small-size crystals. When the crystals become big enough, a high-temperature α process, described as a combination of the inter-lamellar and intra-lamellar motions occurs.

The analysis of the relative intensity of the α relaxation is shown in Figs. 11 and 12. Fig. 11 evidences the poor correlation of the α relaxation intensity with the molar mass. Nevertheless, it is to be noted that the relative intensity of the α relaxation in any iPP family increases when the chain size does so. This is evident in M samples in the whole molar mass range, with a sudden step between 65 000 and 80 000 Da, and less clear in ZN samples because, although a similar abrupt change is found at about 47 000 Da, the high dispersion of values in the highest molar mass samples does not allow to draw an analogous trend to the M case. For the EP family a convergence on the left side with M samples can be supposed.

The sudden step in the evolution of the α relaxation with the molar mass in ZN and M polymers is suggested to be related to a change in the microstructure which must be a determinant. This assumption is made based on the fact that the lower straight line fits the samples with n_1 under 30 units, while samples with n_1 above 30 present values in the upper step. Nevertheless, there are still some points clearly out of this qualitative behaviour. Among them, the case of M125K22 with no α relaxation at all has been mentioned above as likely related either to the crystalline distribution or to the presence of syndiotactic interruptions longer than a triad, or both. Note that ZN46K19 with a similar PP($r_{>2}$) microstructure presents also an almost inexistent α relaxation. More complex is the situation of the two low-molar mass M samples (M16K26 and M29K28) and the two highest ZN samples which, in spite of a similar microstructure (PP(r_2-2,1) and PP(r_2), respectively) and quite analogous molar masses in each case, present completely different intensities of the α relaxation. Crystalline distribution in the M cases and additionally n_1 in the ZN samples can be invoked to account for their deviations. If it turns to be so, these samples can be very useful examples to test the driving influence of n_1 and morphological aspects in this dynamics.

The correlation degree between the α relaxation intensity and the microstructure can be assessed from Fig. 12. As a general remark, a more homogeneous behaviour is apparent for

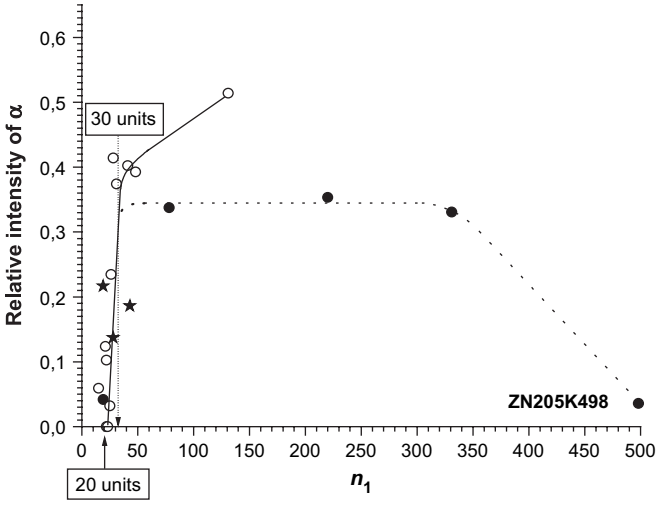

Fig. 12. Evolution of the relative intensity of the α relaxation with n_1: (○) M samples; (●) ZN samples; (★) EP samples.

the three kinds of iPP samples. In agreement with the n_1 dependence of T_α (Fig. 10), two different evolutions are found for ZN and metallocenic polymers, either PP or EP. The strong intensity increase for n_1 up to 30 units must be seen as the effect of the onset of the dynamics. In this way, the behaviour depicted in Fig. 9 can be understood.

Beyond 30 units, the intensity increases gently in M polymers and becomes independent of n_1 in ZN samples around the typical value corresponding to an average isotactic segment of 30 units. These two evolutions match the idea of two α relaxations which are similarly related to the n_1 value, but in a different way, either because of morphological differences between the two families or because of the different role of n_1 itself in each case. As for the ZN205K498 sample, besides morphological differences, a particularly long n_1 could cause the α relaxation intensity to level off. This vanishing effect for very high n_1 would imply the existence of a limiting upper length of the isoregularity, beyond which the exchange between the crystal and the amorphous phase would be hindered. There is also a minimum value required for the α relaxation to take place. Actually, a complete disappearance of the α relaxation occurs when n_1 is under 20 units. This requirement is supposed to cover also the compositional aspect of the microstructure. This is what can be inferred from the study performed by Keating and Lee [39]. The examination of these authors' results evidences the absence of the α relaxation in metallocene ethylene-based copolymers with an ethylene segmental length under 20 units.

3.5. Correlation between α relaxation and crystalline morphology

The preceding analysis proposes microstructure as a factor strongly associated with the quality and the intensity of the α relaxation. Besides this, molar mass appears also somehow connected to the characteristics of the local relaxation. Then, the combined influence of these factors − molar mass and microstructure − could justify a different evolution for ZN and M polymers in Fig. 12 for n_1 longer than 30, as well as the deviation of ZN205K498.

It would be interesting to know how both factors combine their effects to give a satisfactory description of the evolution of the α relaxation intensity. Crystalline distribution is suspected to be the characteristic which resumes the influence of molar mass and microstructure. In fact, the study performed by Alamo et al. [18,35] about the factors which govern the polymorph distribution in metallocene iPP, evidences that interruption content and molar mass are, besides crystallization kinetics, the parameters which control the fraction of low-T_m γ crystals.

The population of low-T_m crystals is proposed to affect greatly the population of free isotactic segments able to be exchanged between the inter-lamellar region and the crystal lattice, as it has been found to occur in the α relaxation [10,13]. It is reasonable to expect a different influence on the local chain transfer of isotactic segments depending on whether low-T_m crystals grow epitaxially or in the radial axis of the spherulite. The former are expected to diminish the folded crystal surface available for the exchange with the amorphous phase to take place, and the latter would play a trapping role which should avoid the transfer.

These influences can be supposed to be general regardless the polymorph type of the low-T_m lamellae, which have been observed to be γ in metallocene iPP [18,31,35] and α in low defective ZN or M iPP chains [30,36].

On the basis of these considerations, the existence of a general correlation between the relative intensity of α dynamics and the relative content of low-T_m crystalline phase has been checked.

The relationship between the relative intensity of the α relaxation and the fraction of the low-T_m crystalline phase is shown in Fig. 13. The correlation is reasonably linear and it includes all the iPP samples with the only deviation of ZN205K498. This behaviour seems consistent with motions which, regardless the exact mechanism, would involve an exchange of isotactic chain segments between the amorphous and the crystalline phases. To summarize, the evolution of Fig. 13 supports the exchange of isotactic segments as the basis of the α relaxation and yields the crystalline distribution as the main parameter to be controlled in order to modulate the intensity of this dynamics. On this matter, a further study using isothermal crystallization conditions will be useful to check the correspondency between thermal and mechanical behaviours. In fact, the content of low-T_m crystalline fraction, for a given sample, is highly dependent on the crystallization temperature [18,26,33,35]. In particular, it would be of interest to verify if the maximum exhibited by the low-T_m fraction, at crystallization temperatures close to the melting point, implies a maximum in the α relaxation intensity.

Among the reasons for the scatter displayed, the multiplicity of the α relaxation and an enhanced error in measuring low intensity processes, in samples with the highest low-T_m crystals content, are suggested to be the main ones. The larger

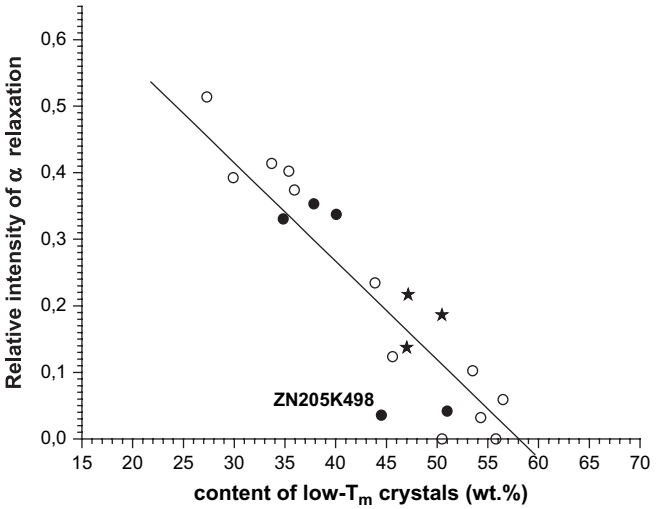

Fig. 13. Relationship between the relative intensity of the α relaxation and the content of low-T_m crystals: (○) M samples; (●) ZN samples; (★) EP samples.

deviation of ZN205K498 cannot be explained at this stage, but a hindered mobility derived from particularly long n_1 in the exchangeable inter-lamellar region could be proposed.

4. Conclusion

This study shows that, apart from special morphological features, microstructure drives strongly the quality of the iPP local α mechanical relaxation. It has been found that n_1 or the total content of interruptions, as equivalent parameters, determines the value of T_α. As for the intensity of the α relaxation, it seems to be mainly controlled by the crystalline distribution, provided that some microstructural requirements are fulfilled (n_1 between 20 and an undetermined value about 500).

It is indeed the combined influence of molar mass and microstructure which, under given processing conditions, determines the fraction of low-T_m crystals, the surface exposed by parent lamellae to the amorphous phase, the trapping degree in the inter-lamellae region and then, the availability of isotactic chains to be exchanged between the amorphous and the crystalline phases, i.e., the occurrence of α motions as they have been described in the literature [10,13].

Acknowledgements

The authors acknowledge the financial support from Comisión Interministerial de Ciencia y Tecnología (CICYT MAT: 2002-04042-C02-02).

References

[1] Tiemblo P, Gómez-Elvira JM, García Beltrán S, Matisova-Rychlá L, Rychlý J. Macromolecules 2002;35:5922.
[2] Olivares N, Gómez-Elvira JM, Tiemblo P. Polym Degrad Stab 1999; 65:297.
[3] Castejón ML, Tiemblo P, Gómez-Elvira JM. Polym Degrad Stab 2001; 71:99.
[4] Tiemblo P, Gómez-Elvira JM, Navarro O, Matisova-Rychlá L, Rychlý J. Polym Degrad Stab 2001;72:23.
[5] Hoyos M, Tiemblo P, Gómez-Elvira JM. Polym Degrad Stab 2006; 91:1433.
[6] Lacey DJ, Dudler V. Polym Degrad Stab 1996;51:101.
[7] Alberola N, Cavaille JY, Perez J. J Polym Sci Polym Phys Ed 1990; 28:569.
[8] Boyd RH. Polymer 1985;26:1123.
[9] Polpli R, Glotin M, Mandelkern L, Benson RS. J Polym Sci Polym Phys Ed 1984;22:407.
[10] Hu WG, Schmidt-Rohr K. Acta Polym 1999;50:271.
[11] Jourdan C, Cavaille JY, Perez J. J Polym Sci Polym Phys Ed 1989; 27:2361.
[12] Read BE. Polymer 1989;30:1439.
[13] Schmidt-Rohr K, Spiess HW. Macromolecules 1991;24:5288.
[14] Van der Ven S. Polypropylene and other polyolefins: polymerization and characterization. Amsterdam: Elsevier; 1990.
[15] Huang J, Rempel GL. Prog Polym Sci 1995;20:459.
[16] Brintzinger HH, Fischer D, Mülhaupt R, Rieger B, Waymouth RH. Angew Chem Int Ed Engl 1995;34:1143.
[17] Kaminsky W. Macromol Chem Phys 1996;197:3907.
[18] Alamo RG, Kim MH, Galante MJ, Isasi JR, Mandelkern L. Macromolecules 1999;32:4050.
[19] Holtrup W. Makromol Chem 1977;178:2335.
[20] Lehtinen A, Paukkeri R. Macromol Chem Phys 1994;195:1539.
[21] Kaminsky W, Engehausen R, Zoumis K. Macromol Chem 1992; 193:1643.
[22] Kurata M, Tsunashima Y. Polymer handbook. 4th ed. New York: John Wiley & Sons; 1999.
[23] Wunderlich B. Macromolecular physics, vol. II. New York: Academic Press; 1976.
[24] Iijima M, Strobl G. Macromolecules 2000;33:5204.
[25] Elvira M, Tiemblo P, Gómez-Elvira JM. Polym Degrad Stab 2004; 83:509.
[26] Auriemma F, De Rosa C. Macromolecules 2002;35:9057.
[27] De Rosa C, Auriemma F, Paolillo M, Resconi L, Camurati I. Macromolecules 2005;38:9143.
[28] Cheng HN. Macromolecules 1984;17:1950.
[29] Busico V, Cipullo R, Corradini P, Landriani L, Vacatello M. Macromolecules 1995;28:1887.
[30] Alamo RG, Brown GM, Mandelkern L, Lehtinen A, Paukkeri R. Polymer 1999;40:3933.
[31] Cheng SZD, Janimak JJ, Rodriguez J. Polypropylene structure: blends and composites, vol. 1. Cambridge: Chapman & Hall; 1995.
[32] Lotz B, Wittmann JC. J Polym Sci Part B Polym Phys 1986;24:1541.
[33] Thomann R, Semke H, Maier RD, Thomann Y, Scherble J, Mülhaupt R, et al. Polymer 2001;42:4597.
[34] De Rosa C, Auriemma F, Di Capua A, Resconi L, Guidotti S, Camurati I, et al. J Am Chem Soc 2004;126:17040.
[35] Hosier IL, Alamo RG, Esteso P, Isasi JR, Mandelkern L. Macromolecules 2003;36:5623.
[36] De Rosa C, Auriemma F, Resconi L. Macromolecules 2005;38:10080.
[37] Zhou H, Wilkes GL. Macromolecules 1997;30:2412.
[38] Jarrigeon M, Chabert B, Chatain D, Lacabanne C, Nemoz G. J Macromol Sci Phys 1980;B17:1.
[39] Keating MY, Lee IH. J Macromol Sci Phys 1999;B38:379.